Published in final edited form as:
Cell Metab. 2014 March 4; 19(3): 512–526. doi:10.1016/j.cmet.2014.01.018.

RBP4 activates antigen-presenting cells leading to adipose tissue inflammation and systemic insulin resistance

Pedro M. Moraes-Vieira[1], **Mark M. Yore**[1], **Peter M. Dwyer**[1], **Ismail Syed**[1], **Pratik Aryal**[1], and **Barbara B. Kahn**[1,2]

[1] Division of Endocrinology, Diabetes and Metabolism, Department of Medicine, Beth Israel Deaconess Medical Center and Harvard Medical School, 330 Brookline Ave., Boston, MA, 02215, USA.

Abstract

Insulin resistance is a major cause of diabetes and is highly associated with adipose tissue (AT) inflammation in obesity. RBP4, a retinol-transporter, is elevated in insulin resistance and contributes to increased diabetes risk. We aimed to determine the mechanisms for RBP4-induced insulin resistance. Here we show that RBP4 elevation causes AT inflammation by activating innate immunity which elicits an adaptive immune-response. RBP4-overexpressing mice (RBP4-Ox) are insulin-resistant and glucose-intolerant and have increased AT macrophage and CD4 T-cell infiltration. In RBP4-Ox, AT $CD206^{+}$ macrophages express pro-inflammatory markers and activate CD4 T-cells while maintaining alternatively-activated macrophage markers. These effects result from direct activation of AT antigen-presenting cells (APCs) by RBP4 through a JNK-dependent pathway. Transfer of RBP4-activated APCs into normal mice is sufficient to induce AT inflammation, insulin resistance and glucose intolerance. Thus, RBP4 causes insulin resistance, at least partly, by activating AT APCs which induce CD4 T-cell Th1 polarization and AT inflammation.

Introduction

The immune system plays an important role in obesity-related insulin resistance which is a major pathogenic factor in type 2 diabetes (T2D) and the related cardiovascular disease (Moraes-Vieira *et al*., 2012; Olefsky and Glass, 2010; Weisberg *et al*., 2003; Xu *et al*., 2002). Large epidemiologic studies demonstrate that elevated circulating RBP4 levels are a biomarker for insulin resistance, prediabetes, the metabolic syndrome (Meisinger *et al*., 2011; Qi *et al*., 2007) and myocardial infarction (Sun *et al*., 2013). Genetic studies indicate that elevated RBP4 markedly increases diabetes risk and may play a causative role in the disease (van Hoek *et al*., 2008). Emerging evidence suggests a possible role for pro-

[2] To whom correspondence should be addressed: 330 Brookline Ave., Boston, MA 02215. Tel.: 617-735-3324; Fax: 617-735-3323; bkahn@bidmc.harvard.edu..

inflammatory pathways in RBP4-induced insulin resistance. RBP4 levels in serum (Balagopal *et al*., 2007) and AT (Yao-Borengasser *et al*., 2007) strongly correlate with subclinical inflammation, including proinflammatory cytokine levels. RBP4 impairs insulin signaling in adipocytes indirectly by inducing pro-inflammatory cytokine production from macrophages through Toll-like receptor 4 (TLR4) and c-Jun N-terminal protein kinase (JNK) pathways (Norseen *et al*., 2012). Also, the RBP4/retinol complex stimulates JAK2/STAT5 signaling and expression of suppressor of cytokine signaling 3, which has also been implicated in insulin resistance (Berry *et al*., 2011).

Several immunologic cell types regulate AT inflammation and insulin sensitivity (Odegaard and Chawla, 2013). Macrophages and dendritic cells (DC), both APCs (Steinman *et al*., 2005), are present in healthy AT throughout the lifespan (Bertola *et al*., 2012; Morris *et al*., 2013). Although leptin, fatty acids, and other factors have been implicated in APC activation, the molecular drivers of AT inflammation are not well understood. AT macrophages (ATMΦ) in healthy AT express anti-inflammatory markers typical of alternatively-activated (AAM), or M2 macrophages, which generally promote tissue repair (Lumeng *et al*., 2007; Odegaard and Chawla, 2013). Obesity triggers the accumulation of $F4/80^{+}$ macrophages in AT (Weisberg *et al*., 2003) which co-express the DC marker CD11c and pro-inflammatory genes typical of classically-activated (CAM), or M1 macrophages (Lumeng *et al*., 2007; Odegaard and Chawla, 2013; Weisberg *et al*., 2003). Recently, AT APCs have been implicated in insulin resistance (Bertola *et al*., 2012; Cipolletta *et al*., 2012; Morris *et al*., 2013). In addition to macrophages, lymphocytes in AT are also regulated by metabolic status (Cipolletta *et al*., 2011; Goossens *et al*., 2012; Lynch *et al*., 2012; Nishimura *et al*., 2009; Strissel *et al*., 2010; Winer *et al*., 2011).

Depending on the signals during the interactions with APCs, CD4 T cells can differentiate into pro- (T helper 1 - Th1 and Th17) or anti-inflammatory (Th2 and regulatory T cells - Treg) cells (Zhu and Paul, 2008). Obesity is associated with a progressive bias toward a pro-inflammatory Th1 phenotype in AT, which is linked to insulin resistance (Winer *et al*., 2009). Moreover, insulin sensitivity is improved in Th1 lineage-defining transcription factor (T-bet) deficient mice on high fat diet (HFD) despite increased visceral adiposity (Stolarczyk *et al*., 2013). The mechanisms that regulate the inflammatory fate of AT T cells are unknown. CD4 T cells undergo polyclonal expansion within AT in obesity (Feuerer *et al*., 2009; Ilan *et al*., 2010; Yang *et al*., 2010). This implies that AT CD4 T cell expansion and polarization are an adaptive immune response to obesity and insulin resistance. Classically, APCs shape CD4 T cell activation by three signals which define the differentiation of naïve CD4 T cells into pro- or anti-inflammatory CD4 T cell subsets: 1) presentation of peptide antigens on major histocompatibility complex class II (MHCII), 2) expression of T cell co-stimulatory molecules (CD40, CD80 and CD86), and 3) production of cytokines. Because RBP4 is elevated in many insulin resistant states (Balagopal *et al*., 2007; Graham *et al*., 2006; Meisinger *et al*., 2011; Qi *et al*., 2007; Yang *et al*., 2005) and data indicate a causative role (van Hoek *et al*., 2008), we proposed that RBP4 triggers AT inflammation *in vivo*. We observed that elevated RBP4 induces APC activation through the JNK pathway which results in pro-inflammatory CD4 T cell proliferation and Th1 polarization. This is sufficient to promote systemic insulin resistance.

Results

RBP4 overexpression results in AT inflammation and systemic insulin resistance

Serum human RBP4 (hRNP4) levels in RBP4-Ox mice were 2-3 fold higher than endogenous mouse RBP4 (data not shown) (Episkopou *et al*., 1993; Quadro *et al*., 2002; Yang *et al*., 2005) and therefore closely represent the serum elevation of RBP4 in insulin resistant ob/ob mice, diet-induced obese mice (Mody *et al*., 2008; Yang *et al*., 2005) and insulin resistant human subjects (Graham *et al*., 2006; Norseen *et al*., 2012; Yang *et al*., 2005) compared to their normal counterparts. RBP4-Ox mice fed on chow diet are glucose-intolerant and insulin-resistant (Figure 1A and 1B) with normal body weight, fat mass, serum triglycerides, free fatty acids and adiponectin (Figure 1C-F). Previously, we showed that RBP4 has a pro-inflammatory effect *in vitro* (Norseen *et. al*., 2012). Because chronic inflammation is a major contributing factor to insulin resistance, we investigated the inflammatory status of the visceral AT of RBP4-Ox mice compared to WT mice. Visceral AT of RBP4-Ox shows more inflammation than WT AT (Figure 1G-I). To characterize visceral AT inflammation, we selected $CD45^+$ cells from AT (Figure S1A) and analyzed the expression of surface markers for specific subtypes of immune cells. First, AT cells were divided in $Ly6C^+Ly6G^-$ cells (monocytes) and $Ly6C^-Ly6G^+$ cells (non-monocyte myeloid cells) (Figure S1A). RBP4-Ox mice have higher numbers of AT monocytes (Figure S1B) which produce higher levels of pro-inflammatory cytokines including TNF and IL-6 (Figure S1B). Next, we evaluated the population of ATMΦ by selecting the $F4/80^+CD11b^+$ cells that were negative for the monocytic marker Ly6C. Back gate analysis of these $CD11b^+F4/80^+$ AT cells revealed that the majority of ATMΦ were $Ly6G^+$ (Figure S1C). Hence, we considered ATMΦ the cells with the phenotype of $CD45^+Ly6C^-Ly6G^+CD11b^+F4/80^+$. RBP4-Ox mice displayed more ATMΦ than WT littermates (Figure 1G). Because the population of $Ly6G^+$ cells (enriched with ATMΦ) is also increased in RBP4-Ox this results in a 70% increase in ATMΦ compared with WT (Figure 1G). These ATMΦ produced higher levels of TNF and IL-1β (Figure 1H), indicating that RBP4 overexpression results in increased AT inflammation. Since Ly6G is also a neutrophil marker, we evaluated the number of neutrophils present in these AT samples. Because neutrophils do not express MHCII, we selected cells that are negative for this marker. To exclude macrophages from this MHCII null population, we further selected for cells negative for the macrophage markers, F4/80 and CD68 and subsequently, cells negative for CD11c and CD206. After these gate exclusions, neutrophils were identified by Gr-1 and CD11b expression (Figure S1D). RBP4-Ox mice do not have increased numbers of neutrophils compared to WT littermates (Figure S1E). To further understand the inflammatory changes in RBP4-Ox mice, we evaluated ATMΦ subpopulations. Pro-inflammatory macrophages have increased CD11c and reduced CD206 expression and anti-inflammatory macrophages have the opposite (Ferrante, 2013; Lumeng *et al*., 2007; Nguyen *et al*., 2011) (Figure 1I, top panel). RBP4-Ox mice displayed a 5-fold increase of $CD11c^+$ and a 60% increase in $CD206^+$ macrophages (Figure 1I, bottom panel). However, $CD206^+$ macrophages were still more abundant in AT of both genotypes. Together, our data indicate that RBP4-Ox have increased numbers of macrophages of two distinct subtypes, $CD11c^+$ and $CD206^+$.

RBP4 overexpression enhances antigen presentation capacity in adipose tissue macrophages

Because RBP4-Ox ATMΦ produce more CD4 T cell-activating cytokines (Figure 1H), we evaluated the population of these cells in RBP4-Ox AT and found increased numbers of CD4 T cells (Figure 2A).

Although obesity and insulin resistance are usually associated with reduction in Treg cells (Cipolletta *et al*., 2011), lean RBP4-Ox mice did not show any difference in AT Treg numbers and percentages (Figure 2B). However, there were more memory ($CD4^+CD44^+$) and activated ($CD4^+CD69^+$) T cells in AT of RBP4-Ox mice (Figure 2C). RBP4-Ox had increased percentage and number of $CD4^+$ T cells producing IFN-γ (Th1) (Figure 2D). No differences in the population of Th2 ($CD4^+IL\text{-}4^+$) and Th17 ($CD4^+IL\text{-}17^+$) cells were observed (Figure S2A-B). Next, we evaluated MHCII and co-stimulatory molecules (CD86 & CD40) required for ATMΦ-mediated CD4 T cell activation and found they were significantly increased in RBP4-Ox ATMΦ (Figure 2E). This elevation was specific to $CD206^+$ ATMΦ (Figure 2G) as no elevation in MHCII, CD86 or CD40 was observed in $CD11c^+$ ATMΦ (Figure 2F). Thus, RBP4-Ox mice have not only a higher number of $CD11c^+$ and $CD206^+$ ATMΦ, but more of the $CD206^+$ ATMΦ are likely to induce CD4 T cell activation compared with WT $CD206^+$ ATMΦ. This is further demonstrated in Figure 4.

RBP4 overexpression results in mild liver inflammation but not systemic inflammation

To determine whether increased ATMΦ and CD4 T cell numbers in RBP4-Ox mice are localized (specific to perigonadal/visceral AT) or systemic, we analyzed the spleen, mesenteric lymph node (data not shown), subcutaneous adipose tissue and liver of RBP4-Ox mice compared to WT littermates. The increased number of AT $CD4^+$ T cells producing IFN-γ (Th1) was specific to visceral AT as no increase in Th1 cells was observed in the spleen and lymph node of RBP4-Ox mice compared to WT littermates (Figure S2C-D). Moreover, no difference was observed in the numbers or percentages of total CD4 T cells, Treg cells (data not shown), monocytes, macrophages or DCs (Figure S3A-E). Furthermore, no difference in the expression of MHCII and co-stimulatory molecules in splenic dendritic cells and macrophages were found (Figure S3F and S3G). We next evaluated whether the subcutaneous AT of RBP4-Ox mice displayed signs of inflammation. No increase in the inflammatory markers CD11c, TNF, and IL-6 and of Arg-1 was observed in subcutaneous AT (Figure S4A). Moreover, no change in the total number of $CD11c^+$ or $CD206^+$ macrophages or CD4 T cells were observed (Figure S4B-D). However, liver of RBP4-Ox mice displayed a modest increase in TNF expression compared to control littermates (Fig 3A). Flow cytometry analysis of these liver samples showed elevated numbers of total liver macrophages (Figure 3B) consisting of three different phenotypes: $CD11c^+$, $CD206^+$, and $CD11c^+CD206^+$ (Figure 3C) and higher numbers of macrophages expressing TNF, but not IL-1β were detected (Figure 3D). In contrast to ATMΦ (Figure 2E-G), liver macrophages from RBP4-Ox mice did not display increased levels of MHCII and CD40 compared to WT macrophages (Figure 3E). In agreement with these results, no difference in the total number of CD4 T cells or in the percentage or total number of Th1 cells was observed (Figure 3F). To understand whether the differences in liver and AT inflammation could be due to different RBP4 levels in these tissues, we measured transgenic human RBP4 in RBP4-Ox

mice. Human RBP4 was 6-fold higher in perigonadal adipose tissue compared to liver (Figure 3G). The endogenous mouse RBP4 levels in serum, liver and adipose tissue were not altered by hRBP4 overexpression (Figure 3H). These data indicate that increased RBP4 levels promote the accumulation of both $CD11c^+$ and $CD206^+$ macrophages in perigonadal AT and liver, but not in peripheral lymphoid tissues or subcutaneous fat and that RBP4-induced CD4 T cell responses take place preferentially in perigonadal AT possibly due to increased hRBP4 levels in adipose tissue compared to liver.

RBP4 overexpression causes $CD206^+$ adipose tissue macrophages to express pro-inflammatory molecules

Since our data indicate that RBP4 overexpression promotes $CD11c^+$ and $CD206^+$ ATMΦ accumulation (Figure 1I), we performed immunophenotyping both ATMΦ subtypes. ATMΦ were FACS-sorted by surface markers into $CD11c^+$ ($Ly6C^-CD11b^+F4/80^+CD11c^+CD206^-$) or $CD206^+$ ($Ly6C^-CD11b^+F4/80^+CD11c^-CD206^+$) positive populations. The expression of other markers enriched in classically-activated and alternatively-activated macrophages (Ferrante, 2013; Han *et al*., 2013; Nguyen *et al*., 2011) were evaluated to verify ATMΦ polarization (Figure 4A). RBP4 overexpression increased the expression of classically-activated macrophage related markers in $CD206^+$ ATMΦ to levels similar (TNF) and even higher (IL-1β and IL-12) than in $CD11c^+$ ATMΦ (Figure 4A) without decreasing the expression of alternatively-activated macrophages related markers (Figure 4B). These data confirm that RBP4 overexpression up regulates pro-inflammatory cytokines in ATMΦ that express alternatively-activated macrophage markers.

Adipose tissue $CD206^+$ macrophages of RBP4-Ox are potent inducers of Th1 T cells

ATMΦ are sufficient to induce CD4 T cell proliferation (Morris *et al*., 2013). Thus, we next measured the capacity of purified AT $CD11b^+$ cells (enriched with ATMΦ) to trigger CD4 T cell proliferation. $CD11b^+$ cells from RBP4-Ox mice induced higher proliferation of CD4 T cells compared to WT $CD11b^+$ cells (Figure S5A). To determine whether both $CD11c^+$ and $CD206^+$ ATMΦ induce CD4 T cell proliferation, we FACS-sorted ATMΦ and co-cultured them with syngeneic WT splenic CD4 T cells. $CD11c^+$ and $CD206^+$ macrophages from both WT and RBP4-Ox mice induced higher proliferation of CD4 T cells compared with total myeloid ($CD11b^+$) cells (Figure S5B). $CD11c^+$ and $CD206^+$ ATMΦ from RBP4-Ox mice induced greater proliferation of CD4 T cells compared to WT ATMΦ (Figure 4C and 4D). Importantly, $CD206^+$ ATMΦ from RBP4-Ox mice induced greater CD4 T cell proliferation than $CD11c^+$ ATMΦ from WT and RBP4-Ox mice and $CD206^+$ ATMΦ from WT mice (Figure 4C and 4D).

To determine whether these ATMΦ also affect CD4 T cell polarization, the intracellular cytokine content of co-cultured CD4 T cells was measured. Although both $CD11c^+$ and $CD206^+$ ATMΦ from RBP4-Ox and WT mice were unable to induce Th17 polarization (Figure S5C), they induced Th1 T cell polarization (Figure 4E and 4F). No difference in the induction of Th1 cells was observed between CD4 T cells co-cultured with $CD11c^+$ ATMΦ from WT compared to RBP4-Ox mice. In contrast, $CD206^+$ ATMΦ from RBP4-Ox mice induced higher percentage of Th1 cells compared to WT $CD206^+$ ATMΦ (Figure 4E-F) and higher proliferation of Th1 cells (Figure S5D). IFN-γ production, characteristic of Th1 cells,

by CD4 T cells was higher when they were co-cultured with $CD206^+$ ATMΦ from RBP4-Ox mice compared with $CD206^+$ from WT mice (Figure 4G). No polarization to Th2 or Th17 was observed in the co-culture assay as indicated by lack of IL-4 or IL-17 secretion (data not shown). To further confirm Th1 polarization, we measured CD4 T cell lineage transcription factor (Tbx21) expression in co-cultured cells. *Tbx21* was up-regulated in the co-culture of $CD206^+$ ATMΦ from RBP4-Ox with CD4 T cells compared to $CD206^+$ ATMΦ from WT mice and compared to $CD11c^+$ ATMΦ from both genotypes (Figure 4H). This was reinforced by increased AT *Tbx21* expression in RBP4-Ox compared to WT mice (Figure S5E). Th2 (*Gata-3*), Th17 (*Rorc*) and Treg (*Foxp3*) transcription factor expression were unchanged. These results indicate that $CD206^+$ ATMΦ from RBP4-Ox mice retain their alternatively-activated macrophage phenotype, but potently activate and promote a pro-inflammatory Th1 profile.

RBP4 directly activates antigen presentation by antigen-presenting cells

We wanted to determine whether treatment of APCs with RBP4 is sufficient to cause insulin resistance *in vivo*. Because i) both macrophages and dendritic cells are professional antigen presenting cells, ii) the yield of bone marrow derived dendritic cells (BMDC) is much greater than bone marrow derived macrophages (BMDM) and iii) dendritic cell transfer systems are far better worked out than macrophage transfer systems (Quintana *et al*., 2010; Ruffner and Robbins, 2010; Sivaganesh *et al*., 2013), we activated BMDC with RBP4 for *in vivo* transfer experiments. RBP4 potently activated BMDC in a dose dependent manner as evidenced by up regulation of MHCII, co-stimulatory molecules (Figure 5A and Figure S5F) and of pro-inflammatory cytokines (Figure 5B). The induction of IL-12 was confirmed by intracellular staining in $CD11c^+MHCII^+$ BMDC (Figure 5C). Moreover, RBP4-activated BMDC induced CD4 T cell proliferation (Figure 5D and 5E). RBP4-activated BMDC co-cultured with CD4 T cells resulted in increased IFN-γ secretion (Figure 5F) and IFN-γ and TNF intracellular staining in CD4 T cells (Figure 5G), indicative of Th1 T cell polarization. There was no induction of other CD4 T cell subtypes indicated by reduced IL-4 and IL-17 intracellular staining (Figure 5G). These results were confirmed by increased expression of *Tbx21* and not of *Gata-3*, *Rorc* and *Foxp3* (Figure 5H). Thus, RBP4 directly activates BMDCs and causes Th1 polarization. The RBP4 effects on CD4 T cells are mediated by activation of APCs, as RBP4 has no direct effect on splenic CD4 T cells in both WT and RBP4-Ox mice (Figure S5G). Proteomic and lipidomic mass spectrometry analysis of our RBP4 preparation confirmed its purity and showed no contaminating endotoxin (LPS), other lipopolysaccharides, lipoproteins, lipids or additional proteins (Figure S6A-B, Norseen et al., 2012). Absence of potential lipopolysaccharide contamination is further demonstrated by the fact that boiling, which would denature the RBP4 protein, removed the effect of RBP4 to stimulate TNF secretion from BMDC, but not the effect of LPS (Figure S6C). If LPS was present, the pro-inflammatory effect of RBP4 would persist after boiling. In addition, recombinant RBP4 generated from mammalian cells (Figure S6D) and hRBP4 purified from human blood (data now shown), where the potential exposure to LPS is minimal, had the same inflammatory effect as bacterially-derived RBP4. A summary of the data confirming the purity of our RBP4 preparation is shown in Table S1.

Transfer of RBP4-activated APCs into WT mice leads to adipose tissue inflammation and insulin resistance

To determine whether RBP4 activation of APCs is sufficient to cause AT inflammation and insulin resistance, we performed APC transfer experiments. Control (not activated) immature dendritic cells (iDC) and RBP4-activated mature dendritic cells (mDC) were transferred into lean, WT mice. Transfer of mDC but not iDC or PBS alone resulted in insulin resistance (Figure 6A-B). Transfer of RBP4-activated BMDC (mDC) also resulted in elevated fasting glucose levels (Figure 6C), glucose intolerance (Figure 6D-E), and increased insulin levels (Figure 6F) with no change in body weight or adiponectin levels (Figure 6G). Moreover, mDC transfer resulted in increased ATMΦ and ATMΦ-producing pro-inflammatory cytokines (Figure 6H). A switch between a predominant $CD206^+$ phenotype to a $CD11c^+$ phenotype occurred when mice received mDC (Figure 6I). Because RBP4 activates APCs and increases their capacity to activate CD4 T cells, we analyzed the AT CD4 T cell profile. Transfer of mDC resulted in increased numbers of total CD4 T cells and CD4 T cells producing IFN-γ and TNF (Figure 6J-K). Thus, BMDC activation by RBP4 is sufficient to cause AT inflammation and insulin resistance in normal mice.

RBP4-induced activation of macrophages and antigen presentation to CD4 T cells is partially dependent on JNK signaling

Previously we showed that the JNK pathway is important for RBP4-induced macrophage activation *in vitro* (Norseen *et al*., 2012). JNK1 and JNK2 in macrophages are required for induction of AT inflammation and insulin resistance in obesity (Han *et al*., 2013). Therefore, we analyzed the activation status of JNK in $CD45^+CD11b^+$ AT cells (myeloid cells) in both RBP4-Ox and WT mice. RBP4-Ox mice display increased phosphorylation of JNK in $CD45^+CD11b^+$ cells compared to WT mice (Figure 7A). In addition, RBP4 effects on macrophages and dendritic cells are STRA6-independent since these cells do not express STRA6 (Figure S7A). Furthermore, RBP4-induced cytokine/chemokine (TNF, IL-6, IL-12, IL-1β, IFN-γ and MCP1), MHCII, and co-stimulatory molecule levels were significantly reduced in both JNK 1/2 KO BMDM compared to WT BMDM and in WT BMDM in the presence of JNK inhibitor (Figure S7B-C).

To assess JNK involvement in AT $CD11c^+$ and $CD206^+$ macrophages, we FACS-sorted $CD11c^+$ and $CD206^+$ macrophages from WT mice and stimulated them *in vitro* with RBP4 in the presence or absence of JNK inhibitor. RBP4 upregulated TNF, IL-6, IL-12 and IL-1β in both $CD11c^+$ and $CD206^+$ macrophages equally (Figure 7B), indicating activation of both populations of cells. Treatment with JNK inhibitor reduced the RBP4-induced upregulation of cytokines in both $CD11c^+$ and $CD206^+$ macrophages (Figure 7B), indicating that RBP4 activation of both populations of macrophages in partially JNK dependent. Next, we sorted $CD11c^+$ and $CD206^+$ macrophages from JNK1/2 KO and control WT mice and treated them *in vitro* with RBP4. With the exception of IL-6, RBP4 induced the secretion of TNF, IL-12 and IL-1β in both $CD11c^+$ and $CD206^+$ ATMΦ from WT mice to similar levels (Figure 7C). However, JNK1/2 KO $CD11c^+$ and $CD206^+$ ATMΦ displayed decreased secretion of these cytokines (Figure 7C), with a complete block in RBP4-induced IL-6 and IL-1β secretion.

Because JNK ablation inhibited RBP4-induced activation of AT macrophages, we next investigated the outcome of this inhibition on CD4 T cell proliferation and Th1 polarization. RBP4-activated $CD11c^+$ and $CD206^+$ ATMΦ induce CD4 proliferation and Th1 polarization (Figure 7D-E). RBP4-activated $CD11c^+$ and $CD206^+$ ATMΦ from JNK1/2 KO mice displayed reduced capacity to induce CD4 T cell proliferation (Figure 7D-E) and Th1 polarization compared to WT (Figure 7D-E). Thus, RBP4 activation of both $CD11c^+$ and $CD206^+$ ATMΦ and induction of CD4 T cell activation by both $CD11c^+$ and $CD206^+$ ATMΦ depends on JNK signaling.

Discussion

The mechanisms for RBP4-induced insulin resistance *in vivo* are unknown. Here we show that RBP4 directly activates AT APCs in a JNK-dependent manner, induces $CD206^+$ macrophages to secrete pro-inflammatory cytokines, and triggers CD4 T cell polarization (Th1) and proliferation. Elevation of RBP4 results in greater inflammation in adipose tissue than in liver. In both tissues, the innate immune system (macrophages) is activated but the adaptive immune system (CD4 T cells), which amplifies the inflammation, is activated only in visceral adipose tissue. APC activation by RBP4 is sufficient to cause insulin resistance since transfer of RBP4-activated APCs into normal mice induces AT inflammation and impairs glucose tolerance and insulin sensitivity.

In obesity and other insulin resistant states, AT macrophage polarization spans a spectrum and the optimal constellation of markers to define pro- and anti-inflammatory macrophages is still evolving. Pro-inflammatory ATMΦ which express $CD11c^+$ (used as a marker for classically activated, also called M1 macrophages) are generally increased leading to inflammation-induced insulin resistance (Lumeng *et al*., 2007). This results in a reduction in the relative number of $CD206^+$ macrophages (alternatively-activated or M2 macrophages) which are predominantly anti-inflammatory (Fujisaka *et al*., 2009; Han *et al*., 2013; Lumeng *et al*., 2007; Stein *et al*., 1992). In AT of RBP4-Ox mice, not only $CD11c^+$ macrophages, but also $CD206^+$ macrophages are increased. In addition, in RBP4-Ox AT, $CD206^+$ macrophages unexpectedly produce pro-inflammatory cytokines and express elevated amounts of co-stimulatory molecules required for CD4 T cell activation which are typical of $CD11c^+$ macrophages (Lumeng *et al*., 2007; Stein *et al*., 1992). Importantly, although these $CD206^+$ macrophages have increased pro-inflammatory cytokine expression, they retain the expression of molecules that are usually associated with alternatively-activated macrophages (Lumeng *et al*., 2007; Odegaard and Chawla, 2011). Because $CD206^+$ macrophages are 20 times more abundant than $CD11c^+$ macrophages in AT of RBP4-Ox mice, the changes in $CD206^+$ macrophages may play a significant role in AT inflammation.

Accumulation of ATMΦ is only part of the immune response that causes insulin resistance. T cells are also recruited to adipose tissue during the development of obesity-related insulin resistance (Feuerer *et al*., 2009; Nishimura *et al*., 2009; Winer *et al*., 2009). We show in RBP4-Ox mice and with RBP4 treatment of immune cells *in vitro* that RBP4-activated $CD11c^+$ and $CD206^+$ ATMΦ induce CD4 T cell proliferation and Th1 polarization. Thus, RBP4 increases the capacity of ATMΦ to induce a CD4 T cell immune response. Moreover, transfer of RBP4-activated APCs into normal mice is sufficient to increase CD4 T cell

numbers, Th1 polarization and systemic insulin resistance. Th1 cells play a critical role in AT inflammation as the knockdown of these cells ($Tbet^{-/-}$) or their product (IFN-γ) reduces AT inflammation and insulin resistance during obesity (Stolarczyk *et al*., 2013; Strissel *et al*., 2010; Winer *et al*., 2009; Yang *et al*., 2010). Although a reduction in anti-inflammatory Treg cells has been implicated in obesity-related insulin resistance (Feuerer *et al*., 2009), lean insulin-resistant RBP4-Ox mice do not display reduced Treg numbers, indicating that the role of Treg cells may differ in lean versus obese insulin-resistant states.

JNK expression in macrophages is required for both AT inflammation and obesity-induced insulin resistance (Han *et al*., 2013). We previously demonstrated that activation of macrophages *in vitro* by RBP4 was dependent on the JNK pathway (Norseen *et al*., 2012). Here we show that JNK signaling is required *in vivo* for RBP4-mediated pro-inflammatory cytokine secretion and for expression of MHCII and co-stimulatory molecules by ATMΦ. Moreover, we show that JNK signaling in RBP4-treated APCs is required for activation of CD4 T cells. In agreement with our results, the JNK pathway has been implicated not only in the accumulation and activation of AT macrophages (Han *et al*., 2013), but also in Th1 immune responses in obesity (Davis, 2000; Dong *et al*., 2000; Dong *et al*., 1998; Wang *et al*., 1994).

RBP4 undoubtedly is not the only AT derived factor that is important for AT inflammation and T2D. For example, leptin and free fatty acids also induce pro-inflammatory cytokine production (Lord *et al*., 1998; Nguyen *et al*., 2007). However, our data identify RBP4 as a key endogenous protein that contributes to AT inflammation and insulin resistance by triggering an interplay of the innate and adaptive immune systems (Figure 7F). These findings conceptually advance our understanding of the integration of different inflammatory pathways in adipose tissue in insulin resistant states and may have therapeutic implications for type 2 diabetes.

Experimental Procedures

Animal studies and measurement of metabolic parameters

Male RBP4-overexpressing (RBP4-Ox) mice on a C57BL6 background were bred with female C57BL6/J mice (Jackson Laboratories) to generate RBP4-Ox mice and control littermates. The RBP4-Ox mice express human-RBP4 under the control of mouse muscle creatine kinase (MCK) promoter and were extensively characterized (Quadro *et al*., 2002). 14-19 week old male mice were used for all studies. Macrophage-specific JNK1/2 knockout male mice (8 weeks old) were provided by Dr. Roger J. Davis and were previously described (Han *et al*., 2013). Body composition was measured by NMR (Echo Medical Systems). Insulin (ITT) and glucose (GTT) tolerance tests were performed in awake mice after a 5-h fast and a 12-h fast, respectively. Blood glucose was determined withusing a One Touch Basic glucometer (Lifescan). Mouse studies were conducted in accordance with federal guidelines. The Institutional Animal Care and Use Committee (Beth Israel Deaconess Medical Center (BIDMC), Boston, MA) approved all studies. All studies were performed on age- and sex-matched littermates.

Recombinant RBP4 preparation

Human RBP4 was expressed in *Escherichia coli* and purified as described previously (Yang *et al*., 2005). Endotoxin was removed by sequential affinity adsorption to Endotrap matrix (Hyglos GmbH) and Detoxigel (Pierce). Recombinant RBP4 protein purity was determined by Coomassie staining of SDS-PAGE gels and mass-spectrometry with and without a strong cation exchange cleanup.

Generation and RBP4 treatment of bone marrow-derived dendritic cells (BMDC) and macrophages (BMDM)

Mouse bone marrow cells were obtained as previously described (Moraes-Vieira *et al*., 2013b). GM-CSF (R&D) at a concentration of 20 ng/mL was used for BMDC differentiation (Moraes-Vieira *et al*., 2013b). M-CSF at a concentration of 50 ng/mL was used for BMDM differentiation. RBP4 was used at a final concentration of 1, 25 or 50 μg/mL. The dialysate buffer was used as a vehicle control in experiments where indicated. For analysis of cytokine secretion in BMDM and ATMΦ, these cells were pretreated with 5 μM JNK inhibitor (EMD catalog no. 420119) for 30 min and then incubated with RBP4 for 24 hours.

Bead purification, cell sorting and co-culture assay

$CD4^+$ T cells from the spleen of donor C57B6/J male age matched mice and $CD11b^+$ cells from the perigonadal adipose tissue of RBP4-Ox or WT mice were purified by magnetic beads as described by the manufacture (Myotecny). Liver immune cells and AT stromal vascular fractions (SVF) were isolated as previously described (Nguyen *et al*., 2007; Pien and Biron, 2000). AT stromal vascular fractions were stained with fluorescence-labeled antibodies for CD45, CD11b, Ly6C, F4/80, CD11c and CD206 (Biolegend) and sorted at high speed (BD FACSAria II - Beth Israel Deaconess Medical Center Flow Cytometry Core). After sorting, cells purities were higher than 98%.

Flow cytometry of surface markers, intracellular cytokine and Foxp3 transcription factor

The AT stromal vascular fraction or BMDC cells were re-suspended in PBS supplemented with 2% FCS and surface markers were stained with monoclonal antibody for multicolor flow cytometry. For intracellular cytokine staining, cells were stained as previously described (Moraes-Vieira et al., 2013b). To determine the frequency of Tregs ($CD4^+CD25^+Foxp3^+$) *in vivo*, cells were stained intracellular for Foxp3 using a PE anti-mouse/rat Foxp3 antibody kit (eBioscience). The cells were acquired on specially ordered 5 lasers LSR II flow cytometer (BD Biosciences) at the Beth Israel Deaconess Medical Center Flow cytometry Core and analyzed with FlowJo 9.5.3 software (Treestar).

$CD4^+$ T cell proliferation assay

FACS-Sorted $CD11c^+$ ($Ly6C^-CD11b^+F4/80^+CD11c^+CD206^-$) or $CD206^+$ ($Ly6C^-CD11b^+F4/80^+CD11c^+CD206^-$) or bead-purified AT $CD11b^+$ cells or BMDC from WT C57B6/J (not activated - dialysate or activated with RBP4 or LPS) were co-cultured with cell trace violet-labeled bead-purified splenic syngeneic $CD4^+$ T cells from WT mice.

Anti-CD3 antibody (Biolegend) was added. The expansion index was calculated with FlowJo 9.5.3 software.

Gene expression analysis

RNA from M1 and M2 ATMΦ sorted from the AT pooled from 8-10 WT or RBP4-Ox mice was extracted using a RNeasy Mini Kit (Qiagen) according to the manufacturer's instructions. Each sample was run in duplicate and relative expression levels determined using the $2^{-\Delta Ct}$ method with normalization of target gene expression levels to Gapdh (Applied Biosystems).

APC transfer into WT recipient mice

DC were treated with RBP4 (50μg/mL) or vehicle (dialysate). The cells were purified with $CD11c^+$ beads (Miltenyi). BMDC (non-activated – dialysate - iDC) and RBP4-activated BMDC (mDC) were injected i.p. into WT mice (3×10^6 per mouse) once a week for 6 weeks. PBS was injected as control. Three days after the last transfer of BMDC, fasting glucose levels were obtained and 5 days after the last transfer ITT or GTT was performed. The mice were sacrificed one week after the last cell transfer and the perigonadal AT stromal vascular fraction analyzed.

Analytical procedures

Triglyceride levels were measured by colorimetric enzyme assays and free fatty acid levels were measured in serum using the NEFA-C kit (Wako, Richmond, Virginia). Cytokines (Biolegend), adiponectin (Invitrogen) and insulin (Crystal Chem inc.)were measured by ELISA kits. RBP4 tissue and serum levels were measured by Western blot as described (Yang *et al*., 2005).

Statistics

All values are given as means ± S.E.M. Differences among groups were compared using ANOVA with Tukey post-test for multiple comparisons and Student's t-test when there were only two groups. All statistical analyses were performed using GraphPad PRISM® 5 software, and the differences were considered significant when $P<0.05$.

Supplementary Material

Refer to Web version on PubMed Central for supplementary material.

Acknowledgments

We thank Dr. Terry Strom for stimulating discussions; Dr. Diane Mathis and Dr. Aldo Rossini for helpful comments on the manuscript; Dr. Odile D Peroni, Kerry Wellenstein, Abha Dhaneshwar and BIDMC Flow Cytometry Core Facility for technical assistance. We thank Dr. Roger J. Davis and Dr. Myoung S. Han for the macrophage-specific JNK1/2 knockdown mice. We thank the Small Molecule Mass Spectrometry Facility at Harvard University, Dr. Sunia Trauger and Dr. Alan Saghatelian for the mass spectrometry analysis of RBP4. Supported by grants from the National Institute of Health DK RO1 43051 and P30 DK57521 (to BBK); T32 DK grant 2 HD052961-07 (to MY) and a grant from the JPB foundation (to BBK).

References

Balagopal P, Graham TE, Kahn BB, Altomare A, Funanage V, George D. Reduction of elevated serum retinol binding protein in obese children by lifestyle intervention: association with subclinical inflammation. J Clin Endocrinol Metab. 2007; 92:1971–1974. [PubMed: 17341558]

Berry DC, Jin H, Majumdar A, Noy N. Signaling by vitamin A and retinol-binding protein regulates gene expression to inhibit insulin responses. Proc Natl Acad Sci U S A. 2011; 108:4340–4345. [PubMed: 21368206]

Bertola A, Ciucci T, Rousseau D, Bourlier V, Duffaut C, Bonnafous S, Blin-Wakkach C, Anty R, Iannelli A, Gugenheim J, et al. Identification of Adipose Tissue Dendritic Cells Correlated With Obesity-Associated Insulin-Resistance and Inducing Th17 Responses in Mice and Patients. Diabetes. 2012; 61:2238–47. [PubMed: 22596049]

Cipolletta D, Feuerer M, Li A, Kamei N, Lee J, Shoelson SE, Benoist C, Mathis D. PPAR-gamma is a major driver of the accumulation and phenotype of adipose tissue Treg cells. Nature. 2012; 486:549–553. [PubMed: 22722857]

Cipolletta D, Kolodin D, Benoist C, Mathis D. Tissular T(regs): a unique population of adipose-tissue-resident Foxp3+CD4+ T cells that impacts organismal metabolism. Semin Immunol. 2011; 23:431–437. [PubMed: 21724410]

Davis RJ. Signal transduction by the JNK group of MAP kinases. Cell. 2000; 103:239–252. [PubMed: 11057897]

Dong C, Yang DD, Tournier C, Whitmarsh AJ, Xu J, Davis RJ, Flavell RA. JNK is required for effector T-cell function but not for T-cell activation. Nature. 2000; 405:91–94. [PubMed: 10811224]

Dong C, Yang DD, Wysk M, Whitmarsh AJ, Davis RJ, Flavell RA. Defective T cell differentiation in the absence of Jnk1. Science. 1998; 282:2092–2095. [PubMed: 9851932]

Episkopou V, Maeda S, Nishiguchi S, Shimada K, Gaitanaris GA, Gottesman ME, Robertson EJ. Disruption of the transthyretin gene results in mice with depressed levels of plasma retinol and thyroid hormone. Proc Natl Acad Sci U S A. 1993; 90:2375–2379. [PubMed: 8384721]

Ferrante AW Jr. The immune cells in adipose tissue. Diabetes Obes Metab 15 Suppl. 2013; 3:34–38.

Feuerer M, Herrero L, Cipolletta D, Naaz A, Wong J, Nayer A, Lee J, Goldfine AB, Benoist C, Shoelson S, et al. Lean, but not obese, fat is enriched for a unique population of regulatory T cells that affect metabolic parameters. Nat Med. 2009; 15:930–939. [PubMed: 19633656]

Fujisaka S, Usui I, Bukhari A, Ikutani M, Oya T, Kanatani Y, Tsuneyama K, Nagai Y, Takatsu K, Urakaze M, et al. Regulatory mechanisms for adipose tissue M1 and M2 macrophages in diet-induced obese mice. Diabetes. 2009; 58:2574–2582. [PubMed: 19690061]

Goossens GH, Blaak EE, Theunissen R, Duijvestijn AM, Clement K, Tervaert JW, Thewissen MM. Expression of NLRP3 inflammasome and T cell population markers in adipose tissue are associated with insulin resistance and impaired glucose metabolism in humans. Mol Immunol. 2012; 50:142–149. [PubMed: 22325453]

Graham TE, Yang Q, Bluher M, Hammarstedt A, Ciaraldi TP, Henry RR, Wason CJ, Oberbach A, Jansson PA, Smith U, et al. Retinol-binding protein 4 and insulin resistance in lean, obese, and diabetic subjects. N Engl J Med. 2006; 354:2552–2563. [PubMed: 16775236]

Han MS, Jung DY, Morel C, Lakhani SA, Kim JK, Flavell RA, Davis RJ. JNK expression by macrophages promotes obesity-induced insulin resistance and inflammation. Science. 2013; 339:218–222. [PubMed: 23223452]

Ilan Y, Maron R, Tukpah AM, Maioli TU, Murugaiyan G, Yang K, Wu HY, Weiner HL. Induction of regulatory T cells decreases adipose inflammation and alleviates insulin resistance in ob/ob mice. Proc Natl Acad Sci U S A. 2010; 107:9765–9770. [PubMed: 20445103]

Lord GM, Matarese G, Howard JK, Baker RJ, Bloom SR, Lechler RI. Leptin modulates the T-cell immune response and reverses starvation-induced immunosuppression. Nature. 1998; 394:897–901. [PubMed: 9732873]

Lumeng CN, Bodzin JL, Saltiel AR. Obesity induces a phenotypic switch in adipose tissue macrophage polarization. J Clin Invest. 2007; 117:175–184. [PubMed: 17200717]

Lynch L, Nowak M, Varghese B, Clark J, Hogan AE, Toxavidis V, Balk SP, O'Shea D, O'Farrelly C, Exley MA. Adipose tissue invariant NKT cells protect against diet-induced obesity and metabolic disorder through regulatory cytokine production. Immunity. 2012; 37:574–587. [PubMed: 22981538]

Meisinger C, Ruckert IM, Rathmann W, Doring A, Thorand B, Huth C, Kowall B, Koenig W. Retinol-binding protein 4 is associated with prediabetes in adults from the general population: the Cooperative Health Research in the Region of Augsburg (KORA) F4 Study. Diabetes Care. 2011; 34:1648–1650. [PubMed: 21617096]

Mody N, Graham TE, Tsuji Y, Yang Q, Kahn BB. Decreased clearance of serum retinol-binding protein and elevated levels of transthyretin in insulin-resistant ob/ob mice. Am J Physiol Endocrinol Metab. 2008; 294:E785–793. [PubMed: 18285525]

Moraes-Vieira PM, Bassi EJ, Araujo RC, Camara NO. Leptin as a link between the immune system and kidney-related diseases: leading actor or just a coadjuvant? Obes Rev. 2012; 13:733–743. [PubMed: 22498577]

Moraes-Vieira PM, Bassi EJ, Larocca RA, Castoldi A, Burghos M, Lepique AP, Quintana FJ, Araujo RC, Basso AS, Strom TB, et al. Leptin modulates allograft survival by favoring a th2 and a regulatory immune profile. Am J Transplant. 2013a; 13:36–44. [PubMed: 23016759]

Moraes-Vieira PM, Larocca RA, Bassi EJ, Peron JP, Andrade-Oliveira V, Wasinski F, Araujo R, Thornley T, Quintana FJ, Basso AS, et al. Leptin deficiency impairs maturation of dendritic cells and enhances induction of regulatory T and Th17 cells. Eur J Immunol. 2013b Epub ahead of print.

Morris DL, Cho KW, Delproposto JL, Oatmen KE, Geletka LM, Martinez-Santibanez G, Singer K, Lumeng CN. Adipose Tissue Macrophages Function as Antigen Presenting Cells and Regulate Adipose Tissue CD4+ T Cells in Mice. Diabetes. 2013; 62(8):2762–72. [PubMed: 23493569]

Nguyen KD, Qiu Y, Cui X, Goh YP, Mwangi J, David T, Mukundan L, Brombacher F, Locksley RM, Chawla A. Alternatively activated macrophages produce catecholamines to sustain adaptive thermogenesis. Nature. 2011; 480:104–108. [PubMed: 22101429]

Nguyen MT, Favelyukis S, Nguyen AK, Reichart D, Scott PA, Jenn A, Liu-Bryan R, Glass CK, Neels JG, Olefsky JM. A subpopulation of macrophages infiltrates hypertrophic adipose tissue and is activated by free fatty acids via Toll-like receptors 2 and 4 and JNK-dependent pathways. J Biol Chem. 2007; 282:35279–35292. [PubMed: 17916553]

Nishimura S, Manabe I, Nagasaki M, Eto K, Yamashita H, Ohsugi M, Otsu M, Hara K, Ueki K, Sugiura S, et al. CD8+ effector T cells contribute to macrophage recruitment and adipose tissue inflammation in obesity. Nat Med. 2009; 15:914–920. [PubMed: 19633658]

Norseen J, Hosooka T, Hammarstedt A, Yore MM, Kant S, Aryal P, Kiernan UA, Phillips DA, Maruyama H, Kraus BJ, et al. Retinol-binding protein 4 inhibits insulin signaling in adipocytes by inducing proinflammatory cytokines in macrophages through a c-Jun N-terminal kinase- and toll-like receptor 4-dependent and retinol-independent mechanism. Mol Cell Biol. 2012; 32:2010–2019. [PubMed: 22431523]

Odegaard JI, Chawla A. Alternative macrophage activation and metabolism. Annu Rev Pathol. 2011; 6:275–297. [PubMed: 21034223]

Odegaard JI, Chawla A. Pleiotropic actions of insulin resistance and inflammation in metabolic homeostasis. Science. 2013; 339:172–177. [PubMed: 23307735]

Olefsky JM, Glass CK. Macrophages, inflammation, and insulin resistance. Annu Rev Physiol. 2010; 72:219–246. [PubMed: 20148674]

Pien GC, Biron CA. Compartmental differences in NK cell responsiveness to IL-12 during lymphocytic choriomeningitis virus infection. J Immunol. 2000; 164:994–1001. [PubMed: 10623849]

Qi Q, Yu Z, Ye X, Zhao F, Huang P, Hu FB, Franco OH, Wang J, Li H, Liu Y, et al. Elevated retinol-binding protein 4 levels are associated with metabolic syndrome in Chinese people. J Clin Endocrinol Metab. 2007; 92:4827–4834. [PubMed: 17878249]

Quadro L, Blaner WS, Hamberger L, Van Gelder RN, Vogel S, Piantedosi R, Gouras P, Colantuoni V, Gottesman ME. Muscle expression of human retinol-binding protein (RBP). Suppression of the visual defect of RBP knockout mice. J Biol Chem. 2002; 277:30191–30197. [PubMed: 12048218]

Quintana FJ, Murugaiyan G, Farez MF, Mitsdoerffer M, Tukpah AM, Burns EJ, Weiner HL. An endogenous aryl hydrocarbon receptor ligand acts on dendritic cells and T cells to suppress experimental autoimmune encephalomyelitis. Proc Natl Acad Sci U S A. 2010; 107:20768–20773. [PubMed: 21068375]

Ruffner MA, Robbins PD. Dendritic cells transduced to express interleukin 4 reduce diabetes onset in both normoglycemic and prediabetic nonobese diabetic mice. PLoS One. 2010; 5:e11848. [PubMed: 20686610]

Sivaganesh S, Harper SJ, Conlon TM, Callaghan CJ, Saeb-Parsy K, Negus MC, Motallebzadeh R, Bolton EM, Bradley JA, Pettigrew GJ. Copresentation of intact and processed MHC alloantigen by recipient dendritic cells enables delivery of linked help to alloreactive CD8 T cells by indirect-pathway CD4 T cells. J Immunol. 2013; 190:5829–5838. [PubMed: 23630361]

Stein M, Keshav S, Harris N, Gordon S. Interleukin 4 potently enhances murine macrophage mannose receptor activity: a marker of alternative immunologic macrophage activation. J Exp Med. 1992; 176:287–292. [PubMed: 1613462]

Steinman RM, Bonifaz L, Fujii S, Liu K, Bonnyay D, Yamazaki S, Pack M, Hawiger D, Iyoda T, Inaba K, et al. The innate functions of dendritic cells in peripheral lymphoid tissues. Adv Exp Med Biol. 2005; 560:83–97. [PubMed: 15932024]

Stolarczyk E, Vong CT, Perucha E, Jackson I, Cawthorne MA, Wargent ET, Powell N, Canavan JB, Lord GM, Howard JK. Improved Insulin Sensitivity despite Increased Visceral Adiposity in Mice Deficient for the Immune Cell Transcription Factor T-bet. Cell Metab. 2013; 17:520–533. [PubMed: 23562076]

Strissel KJ, DeFuria J, Shaul ME, Bennett G, Greenberg AS, Obin MS. T-cell recruitment and Th1 polarization in adipose tissue during diet-induced obesity in C57BL/6 mice. Obesity (Silver Spring). 2010; 18:1918–1925. [PubMed: 20111012]

Sun Q, Kiernan UA, Shi L, Phillips DA, Kahn BB, Hu FB, Manson JE, Albert CM, Rexrode KM. Plasma Retinol-Binding Protein 4 (RBP4) Levels and Risk of Coronary Heart Disease: A Prospective Analysis Among Women in the Nurses' Health Study. Circulation. 2013; 127:1938–1947. [PubMed: 23584360]

van Hoek M, Dehghan A, Zillikens MC, Hofman A, Witteman JC, Sijbrands EJ. An RBP4 promoter polymorphism increases risk of type 2 diabetes. Diabetologia. 2008; 51:1423–1428. [PubMed: 18496666]

Wang J, Beekhuizen H, van Furth R. Surface molecules involved in the adherence of recombinant interferon-gamma (rIFN-gamma)-stimulated human monocytes to vascular endothelial cells. Clin Exp Immunol. 1994; 95:263–269. [PubMed: 7508346]

Weisberg SP, McCann D, Desai M, Rosenbaum M, Leibel RL, Ferrante AW Jr. Obesity is associated with macrophage accumulation in adipose tissue. J Clin Invest. 2003; 112:1796–1808. [PubMed: 14679176]

Winer DA, Winer S, Shen L, Wadia PP, Yantha J, Paltser G, Tsui H, Wu P, Davidson MG, Alonso MN, et al. B cells promote insulin resistance through modulation of T cells and production of pathogenic IgG antibodies. Nat Med. 2011; 17:610–617. [PubMed: 21499269]

Winer S, Chan Y, Paltser G, Truong D, Tsui H, Bahrami J, Dorfman R, Wang Y, Zielenski J, Mastronardi F, et al. Normalization of obesity-associated insulin resistance through immunotherapy. Nat Med. 2009; 15:921–929. [PubMed: 19633657]

Xu H, Hirosumi J, Uysal KT, Guler AD, Hotamisligil GS. Exclusive action of transmembrane TNF alpha in adipose tissue leads to reduced adipose mass and local but not systemic insulin resistance. Endocrinology. 2002; 143:1502–1511. [PubMed: 11897709]

Yang H, Youm YH, Vandanmagsar B, Ravussin A, Gimble JM, Greenway F, Stephens JM, Mynatt RL, Dixit VD. Obesity increases the production of proinflammatory mediators from adipose tissue T cells and compromises TCR repertoire diversity: implications for systemic inflammation and insulin resistance. J Immunol. 2010; 185:1836–1845. [PubMed: 20581149]

Yang Q, Graham TE, Mody N, Preitner F, Peroni OD, Zabolotny JM, Kotani K, Quadro L, Kahn BB. Serum retinol binding protein 4 contributes to insulin resistance in obesity and type 2 diabetes. Nature. 2005; 436:356–362. [PubMed: 16034410]

Yao-Borengasser A, Varma V, Bodles AM, Rasouli N, Phanavanh B, Lee MJ, Starks T, Kern LM, Spencer HJ 3rd, Rashidi AA, et al. Retinol binding protein 4 expression in humans: relationship to insulin resistance, inflammation, and response to pioglitazone. J Clin Endocrinol Metab. 2007; 92:2590–2597. [PubMed: 17595259]

Zhu J, Paul WE. CD4 T cells: fates, functions, and faults. Blood. 2008; 112:1557–1569. [PubMed: 18725574]

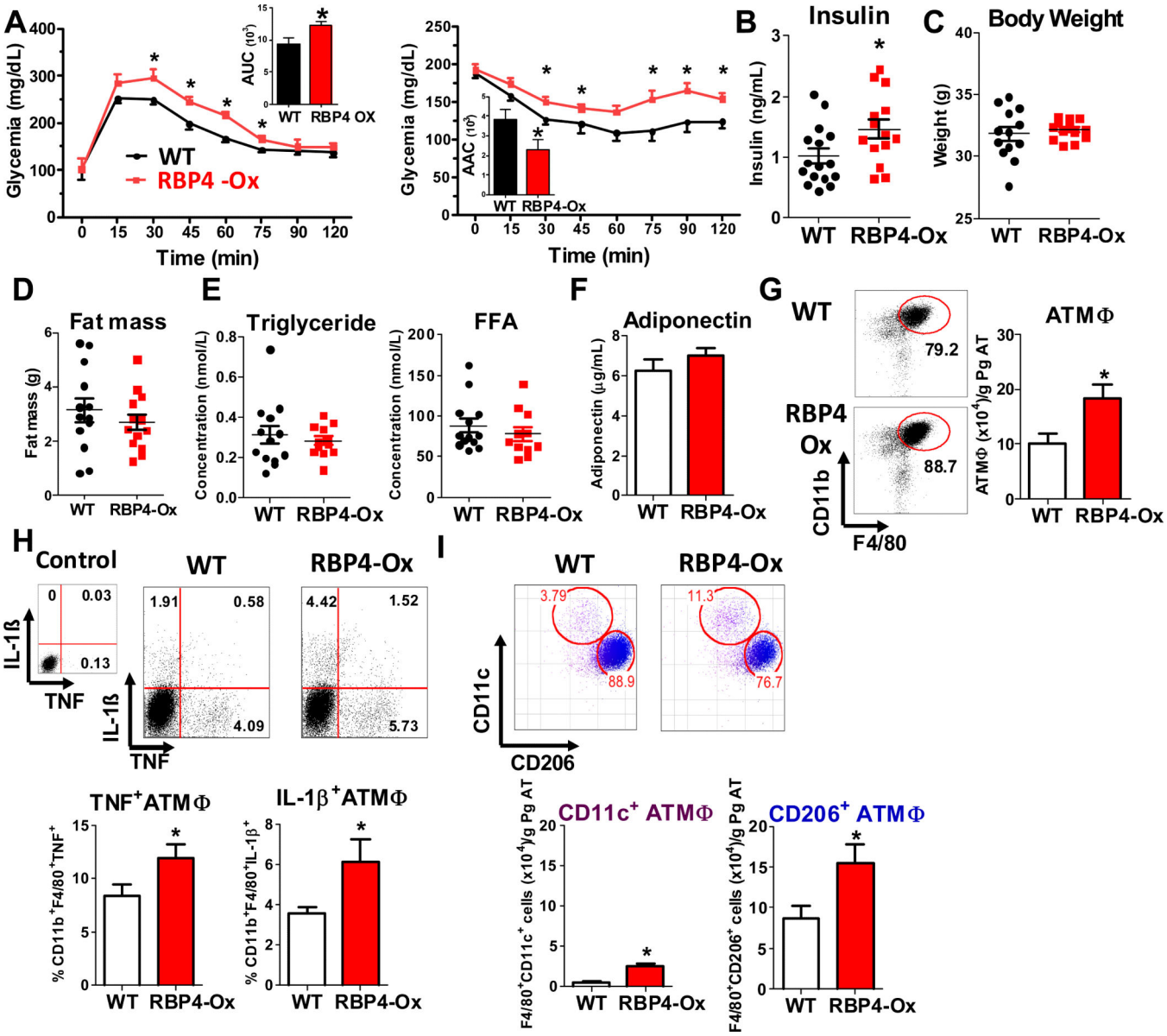

Figure 1. Elevated serum RBP4 levels cause glucose intolerance, insulin resistance and AT inflammation.

(A) Glucose tolerance test (left panel) and insulin tolerance test (right panel) (n=13-15/group). (B) Serum insulin levels (n=13-15/group). (C) Body weight and (D) fat mass (n=13-15/group). (E) Serum triglycerides and free fatty acid (FFA) levels (n=11-13/group). (F) Serum adiponectin levels (n=11-13/group). (G) Flow cytometry representation of gated ATMΦ ($CD11b^+F4/80^+$). ATMΦ numbers in perigonadal fat (right panel) (n=8/group). (H) TNF and IL-1β intracellular staining in ATMΦ (n=5/group). (I) Flow cytometry representation (top panel) and number (botton panel) of $CD11c^+$ and $CD206^+$ ATMΦ (n=8/group). Studies were performed at 12-16 weeks of age. Values are means±standard error. *P<0.05. AUC: area under the curve. AAC: area above the curve. Pg: perigonadal.

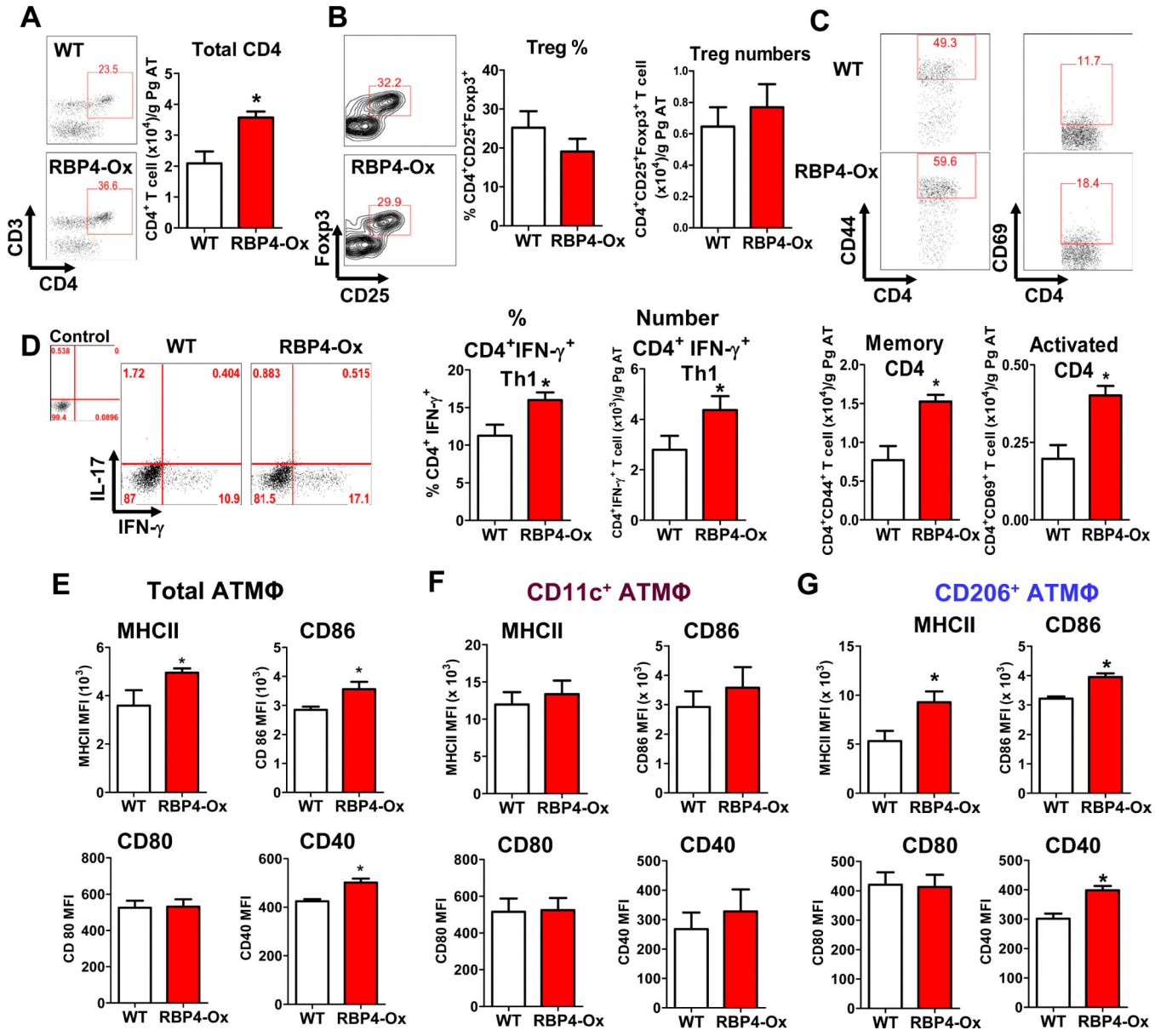

Figure 2. Elevated serum RBP4 levels activate the adaptive immune system in AT

(A) Total $CD4^+$ AT T cell numbers. (B) Flow cytometry representation of gated AT Tregs (left panel) from WT and RBP4-Ox mice. $CD4^+CD25^+Foxp3^+$ AT Treg percentages and numbers (right panel). (C) Flow cytometry representation of gated $CD4^+Foxp3^-CD44^+$ (memory) and $CD4^+Foxp3^{-+}CD69^+$ (activated) T cells (upper panel). Memory and activated CD4 T cell numbers (bottom panels). (D) Flow cytometry representation of gated AT CD4 T cells stained intracellularly with IFN-γ and IL-17 (left panel). Percentage and number of $CD4^+IFN\text{-}\gamma^+$ T cells (right panel). (E) Total $CD11b^+F4/80^+$ ATMΦ from WT and RBP4-Ox were evaluated for the expression of MHCII and co-stimulatory molecules (CD40, CD80 and CD86) by flow cytometry (n=5/group). (F) MHCII and co-stimulatory molecule (CD40, CD80 and CD86) expression in gated $CD11c^+$ (F) and $CD206^+$ (G) ATMΦ. (n=5-6/group). Values are means±standard error. *P<0.05. Pg: perigonadal.

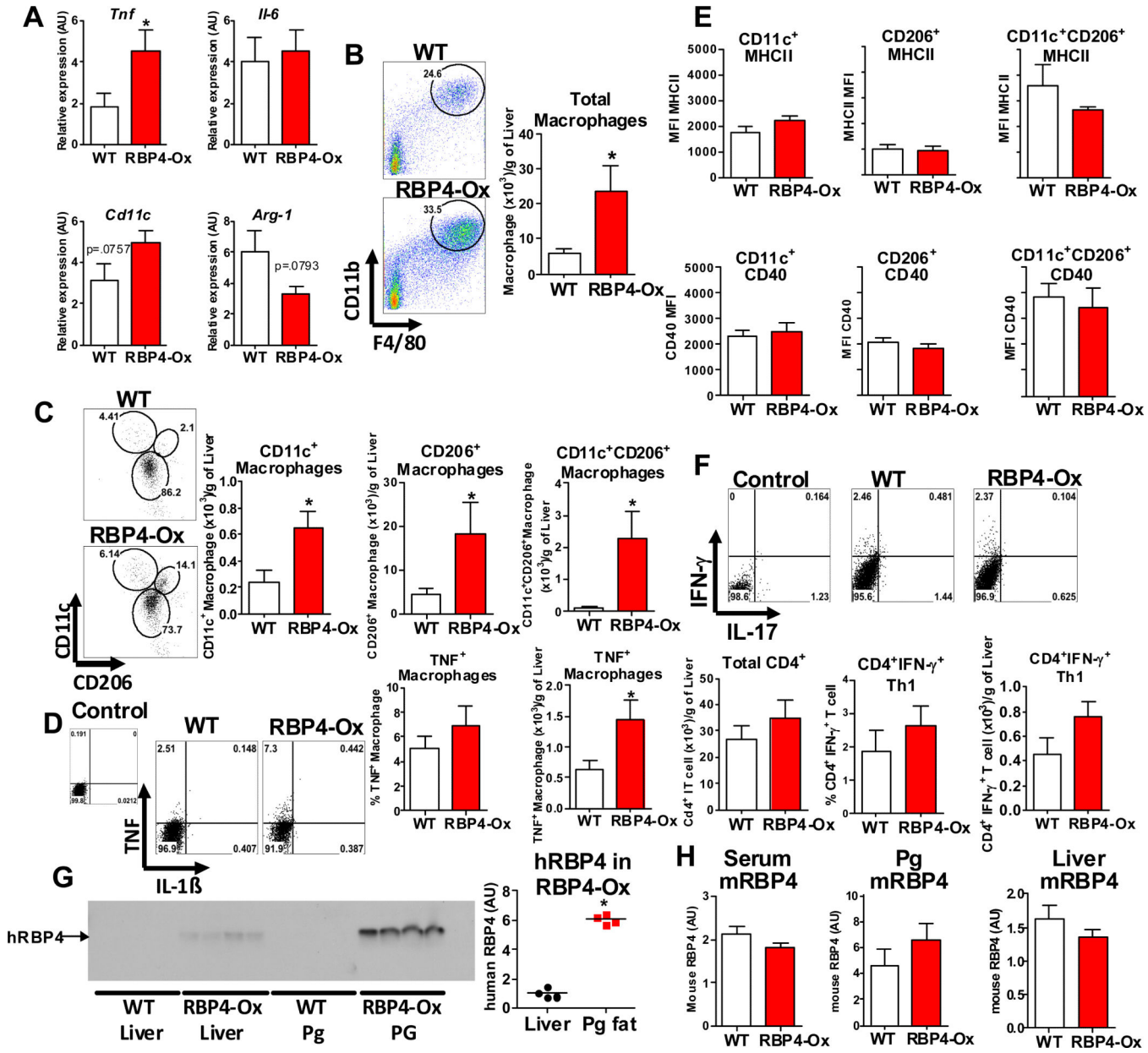

Figure 3. Elevated serum RBP4 levels increase liver macrophage with no effect on CD4 T cell activation.

(A) mRNA expression of Tnf, Il-6, Cd11c and Arg-1 was determined by qPCR. (B) Flow cytometry representation of liver macrophages ($CD11b^+F4/80^+$) gating and macrophage numbers in liver (right panel). (C) Flow cytometry representation (left panel) and number (right panel) of $CD11c^+$, $CD11c^+CD206^+$ and $CD206^+$ liver macrophages. (D) Flow cytometry representation of TNF and IL-1β intracellular staining in liver macrophages (left panel) and percentage and total number of TNF^+ macrophages (right panel). (E) MHCII and co-stimulatory molecule (CD40, CD80 and CD86) expression in gated $CD11c^+$ and $CD206^+$ liver macrophages. (F) Flow cytometry representation of gated AT CD4 T cells stained with IFN-γ and IL-17 (upper panel). Percentage and number of $CD4^+IFN\text{-}\gamma^+$ T cells (bottom

panel). (G) Western blot of transgenic human RBP4 (hRBP4) in AT and liver (left panel) and quantification of blot (right panel). (H) Levels of endogenous mouse RBP4 (mRBP4) in serum, AT and liver of RBP4-Ox and WT mice using an anti-serum that does not cross-react with human RBP4. n=4-6/group. Values are means±standard error. *P<0.05. Pg: perigonadal. MFI: median fluorescence intensity.

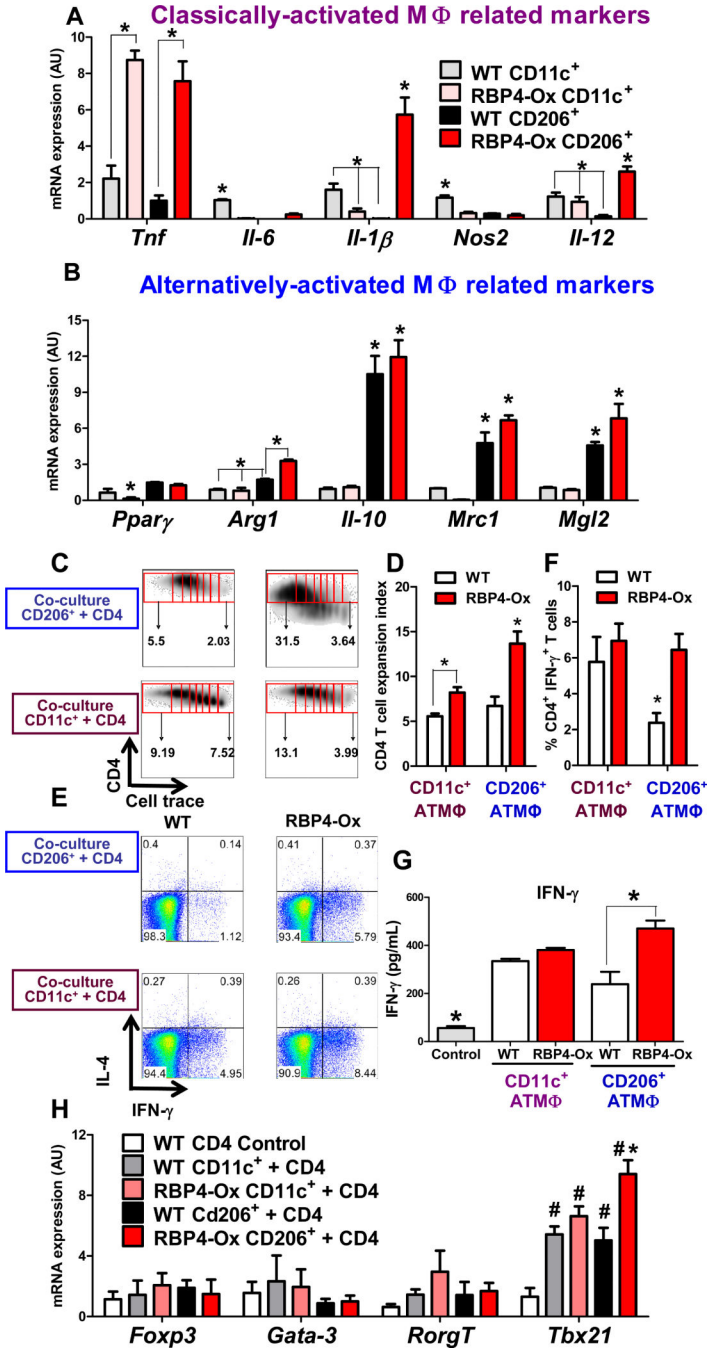

Figure 4. RBP4 overexpression increases proinflammatory markers in CD206$^+$ (alternatively-activated) ATMΦ resulting in Th1 polarization

mRNA expression of classically-activated (A) and alternatively-activated (B) macrophage-related markers in FACS-sorted (98%-purity) CD11c$^+$ and CD206$^+$ Pg ATMΦ from RBP4-Ox and WT mice (n=3 experiments pooling AT from 10-12 mice/group in each experiment). (C) Flow cytometry representation of CD4 T cell proliferation induced by co-culture with CD11c$^+$ and CD206$^+$ ATMΦ. Proliferation was evaluated by cell trace dilution. (D) Expansion index representing the degree of CD4 T cell proliferation. (E) Flow cytometry representation of IL-4 and IFN-γ intracellular staining in CD4$^+$ T cells co-cultured with

$CD11c^+$ or $CD206^+$ ATMΦ. (F) Percentage of IFN-γ^+CD4^+ T cells in the co-culture assay. (G) IFN-γ levels in media from co-culture of $CD11c^+$ or $CD206^+$ ATMΦ with CD4 T cells. (H) mRNA expression in the co-culture assay of CD4 T cell lineage transcription factors. Co-culture assays were performed with FACS-sorted $CD11c^+$ and $CD206^+$ ATMΦ pooled from 6-10 WT or RBP4-Ox mice and incubated with syngeneic splenic CD4 T cells. Values are means±standard error. *$P<0.05$ versus all other groups or as indicated. $^{\#}P<0.05$ vs control. Pg: perigonadal.

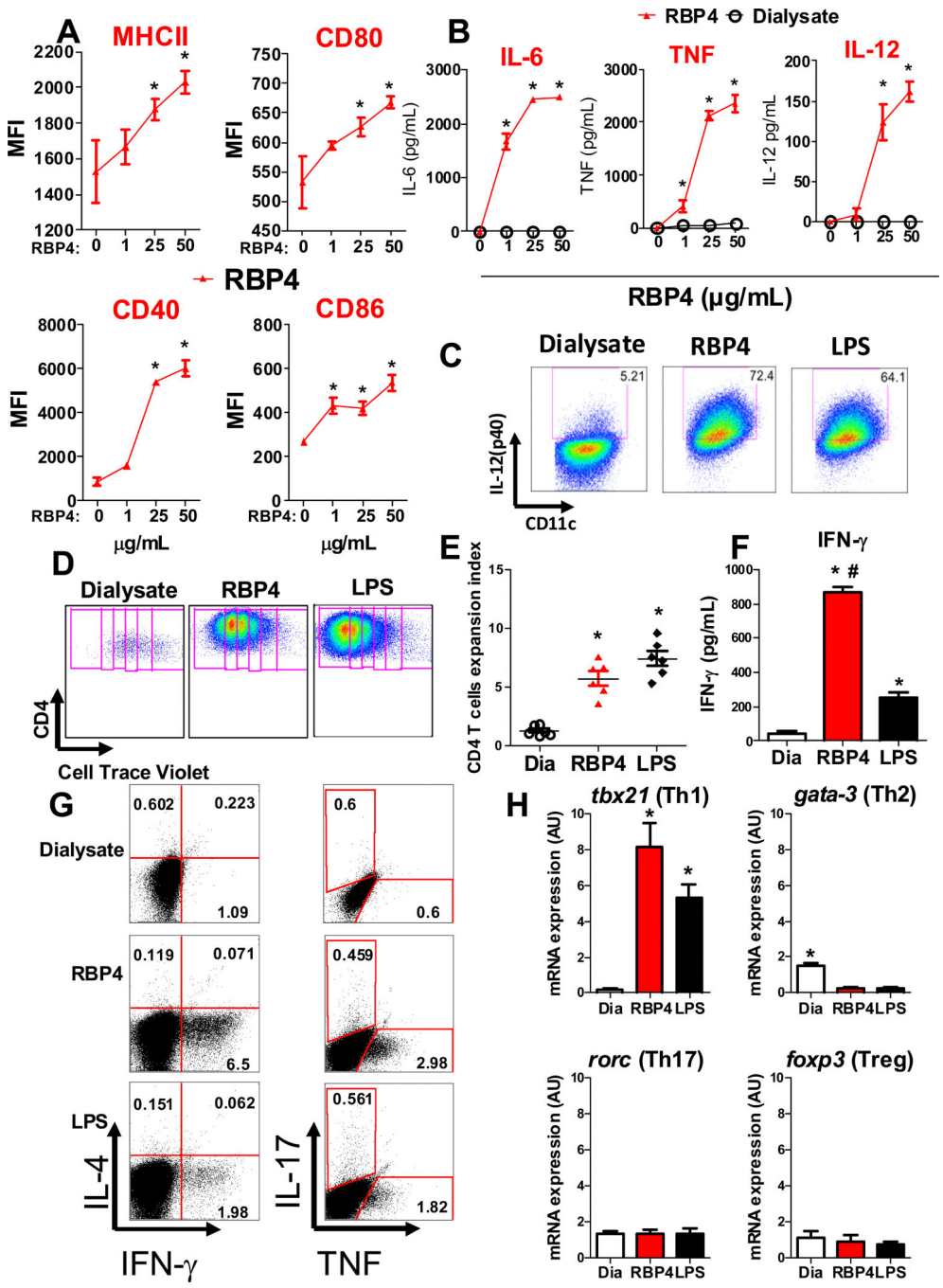

Figure 5. RBP4 directly activates dendritic cells (DCs) which induce CD4 T cell proliferation and polarization

DCs were generated from bone marrow (BMDCs) of 8 week old male WT mice. (A) DC activation was demonstrated by increased expression of CD40, CD80, CD86 and MHCII determined by flow cytometry. (B) Dose response effect of RBP4 on secretion of TNF, IL-6 and IL-12 from BMDCs. (C) Increased production of IL-12 by RBP4- or LPS-activated BMDC was confirmed by intracellular staining of $CD11c^{+}MHCII^{+}$ (BMDCs). (D) RBP4- or LPS-activated BMDCs were co-cultured with splenic syngeneic cell trace-labeled CD4 T cell and CD4 T cell proliferation was demonstrated by cell trace dilution. (E) Expansion

index representing the degree of CD4 T cell proliferation. (F) IFN-γ secretion on day 5 of co-culture. (G) RBP4-activated BMDCs induce IFN-γ and TNF production by CD4 T cells, visualized by intracellular staining using flow cytometry. (H) mRNA expression in the co-culture assay of CD4 T cell lineage transcription factors. Data represent 3 experiments performed in triplicate, each using pools of bone marrow cells from 2-6 mice. *$P<0.05$ versus dialysate. $^{\#}P<0.05$ versus LPS. MFI: median fluorescence intensity. Dia: Dialysate control.

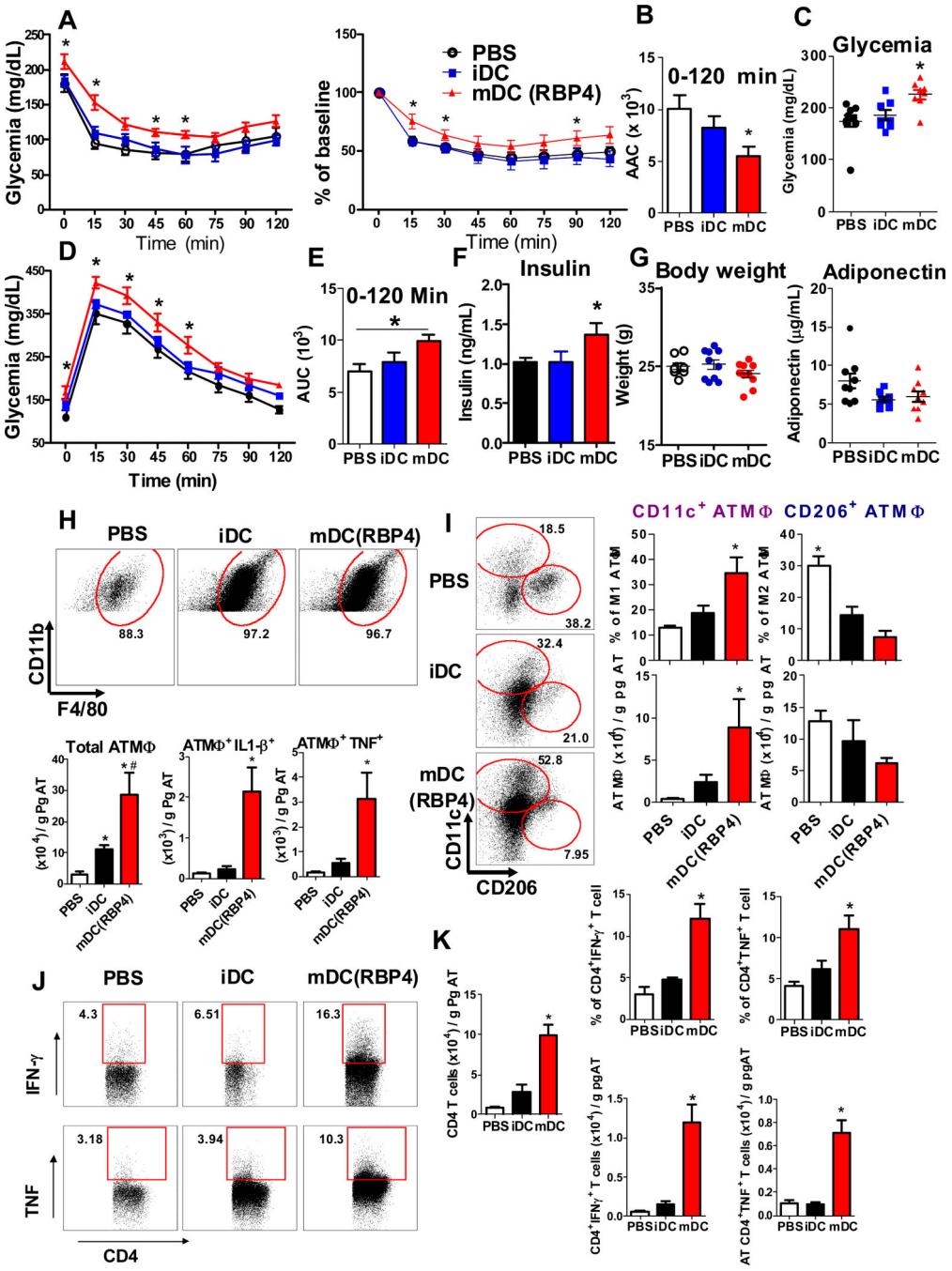

Figure 6. Transfer of RBP4-activated APCs into WT recipient mice causes insulin resistance, glucose intolerance and AT inflammation

DCs were generated from the bone marrow (BMDCs) of WT mice. BMDCs were treated with dialysate (not activated; iDC) or activated with RBP4 (mDC). PBS without cells (control), iDCs or mDCs were injected i.p. in WT mice once a week for 6 weeks. (A) Insulin tolerance test (ITT). (B) Area above the curve of the ITT. (C) Glycemia following food removal. (D) Glucose tolerance test. (E) Area under the curve of the GTT. (F) Serum insulin levels. (G) Body weight and serum adiponectin levels. (H) Flow cytometry representation of gated ATMΦ (upper panel) and total number of ATMΦ and ATMΦ expressing TNF or

IL-1β (bottom panel). (I) Flow cytometry representation of gated $CD11c^+$ and $CD206^+$ ATMΦ (left panel) and percent of $CD11c^+$ and $CD206^+$ ATMΦ (top right). Total number of $CD11c^+$ and $CD206^+$ ATMΦ (bottom right). (J) Flow cytometry representation of gated $CD4^+$, $CD4^+IFN\text{-}\gamma^+$ and $CD4^+TNF^+$ AT T cells. (K) Total AT CD4 T cell numbers (right panel) and $CD4^+IFN\text{-}\gamma^+$ and $CD4^+TNF^+$ AT T cell numbers and percentages. (n=8-10/group for all experiments). Values are means±standard error. $^*P<0.05$ versus all other groups. $^{\#}P<0.05$, mDC versus iDC. Pg: perigonadal.

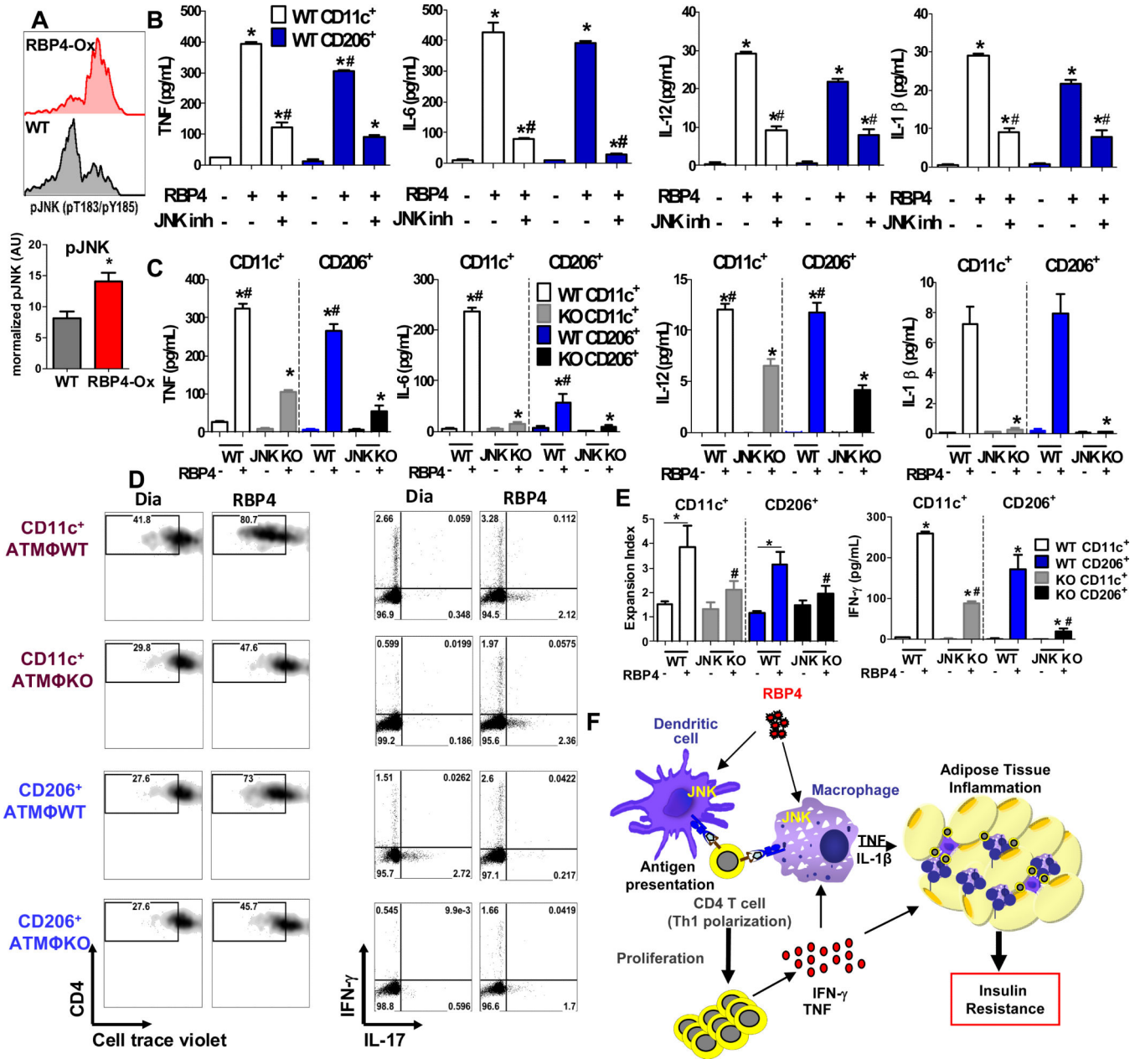

Figure 7. RBP4-induced activation of adipose tissue macrophages and resulting CD4 T cell proliferation and Th1 polarization are JNK-dependent

(A) Histograms representing pJNK staining (pT183/pY185) in CD45$^+$CD11b$^+$ AT cells from RBP4-Ox and WT mice (upper panel) and normalized pJNK levels (bottom panel). (B) CD11c$^+$ and CD206$^+$ ATM were sorted from WT mice and stimulated with RBP4 (50 μg/mL for 24h) in the presence or absence of JNK inhibitor (5μM). Levels of TNF, IL-6, IL-12 and IL-1β were measured by ELISA. (C) CD11c$^+$ and CD206$^+$ ATM were sorted from macrophage specific JNK1/2 knockout (JNK KO) and WT mice and treated with RBP4 (50 μg/mL for 24h). Levels of TNF, IL-6, IL-12 and IL-1β were measured by ELISA. (D) CD11c$^+$ and CD206$^+$ ATM were sorted from JNK KO and WT mice and treated with RBP4 (50 μg/mL for 24h). Next, CD4 T cells plus anti-CD3 antibody were added and CD4

T cell proliferation and IFN-γ^+CD4$^+$ T cells were measured. Flow cytometry representation of CD4 T cell proliferation (left panel) and IFN-γ and IL-17 intracellular staining in gated CD4 T cells (right panel). (E) Expansion index representing the degree of CD4 T cell proliferation (left panel) and IFN-γ^+ secretion in the co-culture assay (right panel) (n=4/group). Values are means±standard error. *P<0.05 versus dialysate control or RBP4 treated. $^{\#}$P<0.05, versus RBP4 treated. Pg: perigonadal. (F) Elevation of RBP4 in serum activates resident ATMΦ and DC and induces pro-inflammatory cytokine secretion and expression of MHCII and co-stimulatory molecules in AT through a JNK-dependent pathway. The pro-inflammatory molecules and cytokines directly contribute to AT inflammation and insulin resistance. These AT APCs induce CD4 T cell proliferation and Th1 polarization resulting in increased levels of TNF and IFN-γ that can activate ATMΦ and further increase AT inflammation and systemic insulin resistance.